

Multipartite entanglement generation and fidelity decay in disordered qubit systems

Simone Montangero^{1,*} and Lorenza Viola²

¹*NEST-INFM & Scuola Normale Superiore, Piazza dei Cavalieri 7, 56126 Pisa, Italy*

²*Department of Physics and Astronomy, Dartmouth College, 6127 Wilder Laboratory, Hanover, NH 03755, USA*

(Dated: July 21, 2022)

We investigate multipartite entanglement dynamics in disordered spin-1/2 lattice models exhibiting a transition from integrability to quantum chaos. Borrowing from the recently introduced generalized entanglement framework, we construct measures for correlations relative to arbitrary local and bi-local spin observables, and show how they naturally signal the crossover between distinct dynamical regimes. In particular, we find that the generation of global entanglement is directly ruled by the local density of states in the short time limit, whereas the asymptotic amount of entanglement is proportional to the degree of delocalization of the chaotic many-body state. Our results are relevant to the stability of quantum information in disordered quantum computing hardware.

PACS numbers: 03.67.Mn, 03.67.Lx, 05.45.Mt, 24.10.Cn

Developing a quantitative understanding of the structural and dynamical properties of entanglement in many-body quantum systems is a critical challenge for both condensed-matter theory and quantum information science. Low-dimensional disordered spin models offer, in this context, an ideal testbed for theoretical analysis. On one hand, these systems are simple enough for analytic benchmarks to exist in limiting situations, yet capable to demonstrate a broad typology of complex quantum phenomena. The latter range from field- or disorder-driven structural ground-state changes responsible for quantum phase transitions [1], to dynamical crossovers from integrable to non-integrable regimes and the emergence of quantum chaos [2]. On the other hand, arrays of interacting spin-1/2 naturally describe a wide class of quantum computing hardware [3], disorder resulting from the unavoidable presence of imperfections in both the single-qubit energy spacings and inter-qubit couplings.

Following [4], considerable effort has been devoted to both assess the impact of disorder on quantum computing performance [5, 6, 7], and to characterize entanglement across the ensuing transition to quantum chaos [8, 9]. These studies point to the key role of spectral properties, as captured by the so-called *Local Density of States* (LDOS) [10], in determining the system stability against the disorder. Changes in the LDOS profile are ultimately responsible for the existence of distinct dynamical regimes – perturbative, Fermi Golden Rule (FGR), and ergodic – as reflected by corresponding changes in the rate of fidelity decay [11]. Numerical experiments [12] confirmed that the same dynamical regimes determine the evolution of pairwise entanglement, as quantified by concurrence [13]. While providing suggestive evidence, the analysis of [12] is unsatisfactory for two reasons. First, concurrence lacks a direct physical interpretation, hindering the possibility to relate entanglement to spectral properties. Second, concurrence is a bipartite measure, preventing the quantification of multipartite correlations which dominate in strongly coupled scenarios.

In this Letter, we overcome the above limitations by exploiting the framework of *Generalized Entanglement* (GE) [14] as a setting for defining entanglement relative to arbitrary sets of observables. In [15], GE measures constructed from algebras of fermionic operators have been applied to the study of broken-symmetry quantum phase transitions in exactly solvable models, notably the spin-1/2 XY chain in a transverse field. Here, we show how GE contributes to the understanding of standard multipartite correlations between distinguishable systems, by selecting *local* and *bi-local* algebras of observables corresponding to individual and pairs of qubits, respectively. Beside providing a transparent physical understanding of all the results based on concurrence [12], our approach allows for quantitative insight about entanglement dynamics starting from arbitrarily correlated initial states. We quantify the explicit influence of LDOS properties in two limits: at short-time, by establishing a direct link with fidelity decay; at long times, by relating the entanglement saturation value to the inverse participation ratio of the asymptotic many-body state.

The model.– We focus on a two-dimensional lattice of n disordered spin-1/2 particles (n even) described, in units $\hbar = 1$, by the following Hamiltonian:

$$H = \sum_{j=1}^n [\Delta + \delta_j] \sigma_z^{(j)} + \sum_{\langle i,j \rangle} J_{ij} \sigma_x^{(i)} \sigma_x^{(j)} \equiv H_\Delta + H_\delta + H_J,$$

where $\sigma_\alpha^{(i)}$, $\alpha \in \{0, x, y, z\}$, $\sigma_0^{(i)} = \mathbb{I}$, denote Pauli operators, and the sum defining H_J runs over nearest-neighbor sites. Open boundary conditions are assumed and, unless otherwise stated, energies are expressed in units of $\Delta \equiv 1$. The parameters δ_j, J_{ij} characterize the disorder in the on-site energy splitting and two-body coupling strengths, respectively. We assume that δ_j, J_{ij} are uniformly random in intervals $[-\delta, \delta]$, $[-J, J]$, with $\delta, J > 0$. The above model, which belongs to the random transverse-field Ising lattice class [16], was recently used to schematize a quantum register with static imperfections [4].

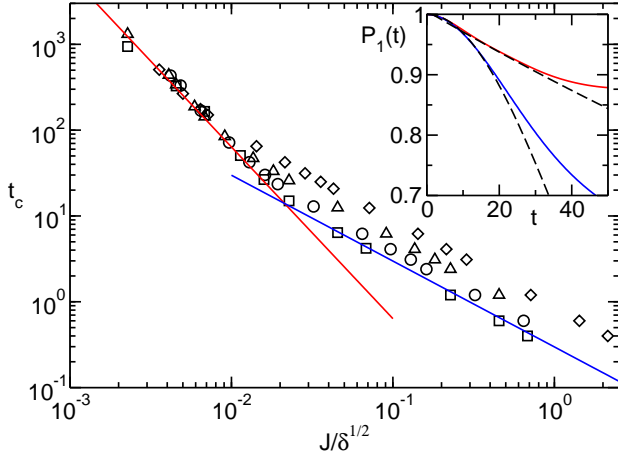


FIG. 1: Local purity critical time t_c ($P_1(t_c) = 0.9$) as a function of $J/\delta^{1/2}$ for $\delta = 0.02, 0.05, 0.1, 0.2$ (diamonds, triangles, circles, squares). To smooth statistical fluctuations, here and in the following we consider averages $\langle P_1(t) \rangle_D$ over a number $N_r = 10$ of disorder realizations. We assume $n = 10$ unless otherwise specified. Inset: Time evolution of $P_1(t)$ in the FGR $J = \delta/10 = 0.01$ (red) and ergodic $J = \delta = 0.1$ (blue) regime starting from the state of Eq. (5) for $n = 14, n_B = 0$. Dotted lines: Exponential and Gaussian fits, as in Eq. (3).

The spectrum of H_Δ is composed of $n + 1$ levels, with energy $E_B = \Delta(2k - n)$ and degeneracy $N_B(k) = n!/[k!(n - k)!]$, $k = 0, \dots, n$. When $\delta, J \ll \Delta$, the degeneration is removed and $n + 1$ bands appears. The width Δ_B of the bands depends on the ratio J/δ [4]. In the limit where $J \ll \delta$, $\Delta_B \sim \delta\sqrt{n}$ as the spread is led by the diagonal term H_δ . Correspondingly, bands are Gaussian. Inside each band, the effective number of states coupled by H_J is given by the width of the LDOS. For $J \lesssim \delta/n \equiv J_c$, H_J couples few states, and the system is slightly perturbed, while for $J > J_c$ quantum chaos sets in and the unperturbed levels are coupled to a quasi-continuum set of states. The LDOS becomes Lorentzian, with a width determined by the FGR, $\Gamma_F = J^2 n/\delta$ [4]. Increasing J , when $\Gamma_F \sim \Delta_B$, that is for $J \sim J_E = \delta/n^{1/4}$, all the levels inside a given band are mixed and the LDOS approaches the level density. Thus, the LDOS becomes a Gaussian with width $\Gamma_E \sim J$ [4]. In summary, three distinct regimes exist – perturbative ($J < J_c$), FGR ($J < J_E$), and ergodic ($J_E < J < \Delta$). It has been shown that starting from an eigenstate $|\psi_0\rangle$ of H_Δ , the survival probability (fidelity henceforth, as for initial eigenstates the fidelity is equivalent to the survival probability) $F(t) = |\langle \psi_0 | \psi_t \rangle|^2$ also follows three different behaviors: $F(t)$ oscillates near one in the perturbative regime, while it decays as an exponential or a Gaussian in the FGR and ergodic regime, respectively [4]. The connection between LDOS shape and fidelity decay has been unveiled in [5] by means of a perturbative relation between $F(t)$ and the Fourier transform of the LDOS.

Local and bi-local purities.— An initial pure state $|\psi_0\rangle$

evolving under H remains pure for any fixed disorder realization. Accordingly, we consider pure-state entanglement throughout. The basic intuition underlying the GE notion [14] is to quantify how entangled a state $|\psi\rangle$ is *relative to an observable set* \mathcal{O} in terms of how pure $|\psi\rangle$ remains upon restricting operational access to \mathcal{O} . While no single set \mathcal{O} can exhaust the complexity of multipartite entanglement, two simple choices will illustrate the usefulness and flexibility of the algebraic approach. First, we consider the set $\mathcal{O} = \mathcal{O}_1$ generated by arbitrary *local* observables that is, we probe the average entanglement of each qubit with the rest of the lattice. The corresponding (time-evolved) *local purity* measure is defined as

$$P_1(|\psi_t\rangle) = \frac{1}{n} \sum_{\alpha=x,y,z}^{i=1,n} |\langle \psi_t | \sigma_\alpha^{(i)} | \psi_t \rangle|^2. \quad (1)$$

For this choice of observables, GE coincides with *global multipartite entanglement* as quantified by the Meyer-Wallach metric Q [15, 17], with $Q = 1 - P_1$ [15, 18]. As a second observable set, whose physical motivation will become clear later, we choose $\mathcal{O} = \mathcal{O}_2$ generated by all the observables acting on pairs of nearest neighbor spins. We compute a *bi-local purity* measure as

$$P_2(|\psi_t\rangle) = \frac{2}{3n} \sum_{\alpha,\beta=x,y,z,0}^{\sim(i,j)} |\langle \psi_t | \sigma_\alpha^{(i)} \sigma_\beta^{(j)} | \psi_t \rangle|^2, \quad (2)$$

where $\langle i, j \rangle$ denotes the underlying lattice partition and the tilde means that the identity term with $\alpha = \beta = 0$ is omitted. Physically, P_2 may be thought as a “coarse-grained” version of P_1 , resulting from ignoring the fine structure given by arbitrary correlations within each pair. Both measures are normalized to give one (zero) on states which are fully separable (contain maximal GE) relative to the corresponding algebra. Remarkably, both P_1 and P_2 are *directly measurable* quantities in principle [18].

Initial separable state.— We first study the generation of multipartite entanglement starting from a separable state in the central band ($k = 0$) that is, $|\psi_0\rangle = |010101\dots 01\rangle \equiv |c\rangle$, where $\{0, 1\}$ label the states of each spin in the computational basis and c is the integer given by the corresponding binary string. The evolution of $P_1(t)$ under different values of J at fixed δ are depicted in the inset of Fig. 1: The decay of $P_1(t)$ clearly follows two different dynamical laws. Specifically, data in the FGR and in the ergodic regime are described, respectively, by

$$P_1^F(t) \approx e^{-C \Gamma_F t}, \quad P_1^E(t) \approx e^{-C' \Gamma_E^2 t^2}, \quad (3)$$

where the constants C, C' depend on the initial state and the lattice coordination number (see e.g. [19]). Let t_c be the time it takes for P_1 (or P_2) to reach the value K e.g., $P_1(t_c) = K$: We find that $t_c^F \sim 1/J^2$ in the FGR regime, whereas $t_c^E \sim 1/J$. These behaviors have been verified over a wide range of disorder parameters, see Fig. 1.

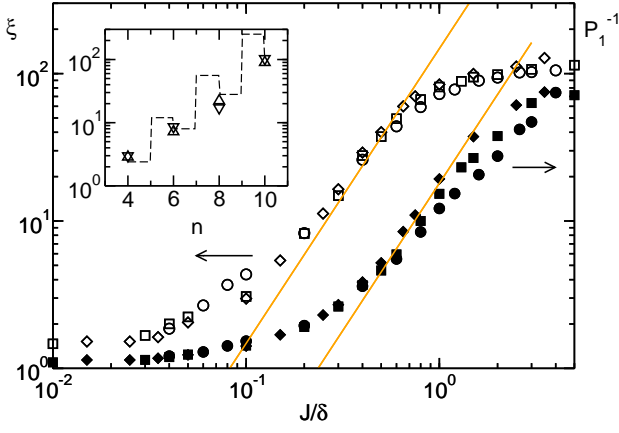


FIG. 2: Saturation values of the IPR (empty symbols) and of the inverse local purity P_1^{-1} as a function of J/δ for $\delta = 0.05$ (circles), $\delta = 0.1$ (squares), $\delta = 0.2$ (diamonds). Straight lines are $C(J/\delta)^2 N_B(0)$, with $C \sim 0.7$ and $C \sim 0.07$. Inset: Saturation value of the IPR (triangles up) and P_1^{-1} (triangles down) in the ergodic regime ($\delta = 0$, $J = 0.1$) as a function of n . The dashed line gives $N_B(0)$ vs n .

A simple physical interpretation of the above results follows from the possibility to directly relate GE dynamics to fidelity decay for any computational eigenstate $|c\rangle$. While a full derivation will be presented elsewhere, the key steps are (i) to realize that only $\sigma_z^{(i)}$ observables contribute to the evolution of $P_1(t)$ (ii) to isolate the fidelity term $|\langle c|e^{-iHt}|c\rangle|^2$ in the resulting z -purity. This yields

$$P_1(t) = F(t)^2 + \frac{1}{n} \sum_{j=1}^n \left(2F(t)(-)^{\pi_j(c)} \alpha_j(t) + \alpha_j(t)^2 \right),$$

where $\alpha_j(t) = \sum_{p \neq c} |\langle p|e^{-iHt}|c\rangle|^2 (-)^{\pi_j(p)}$ and $(-)^{\pi_j(q)} = (-)^{\lfloor q/2^{j-1} \rfloor}$ is the parity of the j th qubit in the computational state $|q\rangle$. One can show that each term $\alpha_j(t)$ is of order $\mathcal{O}((J/\delta)^2 t^2)$. Thus, according to the above equation, the connection between local purity and fidelity decay (hence LDOS via the relation found in [5]) becomes exact in the limit $t \rightarrow 0$. For sufficiently short times, the first term still dominates and the dynamics is governed by $F(t)^2$, whereby the two regimes of Eq. (3) arise.

For times much longer than the decay times $\Gamma_{E,F}$, the GE amount present in the system may be estimated via an appropriate Ansatz for the asymptotic many-body state $|\psi_\infty\rangle$. The following simple model will suffice to our purposes [2]. Assume that $|\psi_\infty\rangle$ is an *approximately* equally-weighted superposition of N_∞ unperturbed states with random phases that is, $|\psi_\infty\rangle = \sum_{p=1}^{N_\infty} e^{i\zeta_p} w_p |p\rangle$, where ζ_p are uniformly random in $[0, 2\pi)$, and $w_p = \bar{w} + \delta w_p$, for \bar{w} , δw_p real. Let w_p be randomly distributed within an interval of width $\Delta w_p = 2f\bar{w}$ centered around \bar{w} , with $0 < f \leq 1$. Thus, the fluctuations have variance $\langle \delta w_p \delta w_q \rangle_D = \delta_{p,q} f^2 \bar{w}^2 / 3$, with $\bar{w} = 1/[\sqrt{N_\infty}(1 + f^2/3)]$. The limit $f \rightarrow 0$

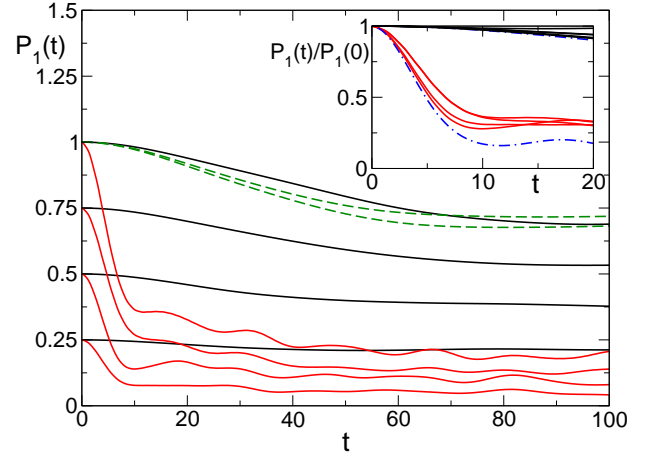


FIG. 3: Local purity $P_1(t)$ versus time in the FGR (black lines) and ergodic regime (red lines) for different initial states with $n_B = 0, 1, 2, 3$, $\delta = 0.1$, and $J = 0.01$ (black curves), $J = 0.1$ (red curves). Dashed lines: Different separable initial states $|\psi_0\rangle = |0101010110\rangle, |010101010\rangle \otimes (|0\rangle + |1\rangle)/\sqrt{2}$ for $\delta = 0.1$, $J = 0.01$. Inset: The same curves rescaled by $P_1(0)$. Also shown (dot-dashed lines) is the local purity decay in the ergodic and FGR regimes for an initial $|w\rangle$ state.

was considered in [12] within a concurrence-based analysis. Including *fluctuations* proves indispensable for a proper description of GE asymptotics. Let the degree of delocalization of $|\psi_\infty\rangle$ be quantified by the so-called *Inverse Participation Ratio* (IPR) [2, 4, 9] ξ that is, $\xi^\infty = 1/\sum_p |e^{i\zeta_p} w_p|^4$. Calculating the disorder-averaged IPR value under the above statistical assumptions yields $\langle \xi^\infty \rangle_D \approx N_\infty(1 - 2\bar{w}^2 N_\infty f^2 - \bar{w}^4 N_\infty^2 f^4/5) \approx N_\infty$, as expected for sufficiently small f ($f^2 \lesssim 1/2$). Because the dynamically accessible states are determined by the ratio between the LDOS width and the bandwidth, one may further estimate that $N_\infty \approx (\Gamma_F/\Delta_B) N_B(0)$ for any initial eigenstate in the central band and in the FGR regime, whereas the IPR is constant in the ergodic regime. These predictions have been confirmed numerically (see Fig. 2). Interestingly, a similar dependence upon $(J/\delta)^2$ has been found for the saturation value of $F(t)$ in [20]. The Ansatz for $|\psi_\infty\rangle$ also determines the asymptotic local purity value as $\langle P_1^\infty \rangle_D \approx 4N_\infty \bar{w}^4 f^2 / 3(1 + f^2/15) \approx 4f^2 / (5N_\infty)$. Thus, we finally obtain the asymptotic GE scaling with $N_B(0)$ and J/δ ,

$$\langle P_1^\infty \rangle_D \propto \frac{1}{\langle \xi^\infty \rangle_D} \propto \frac{\Delta_B}{\Gamma_F N_B}. \quad (4)$$

As seen in Fig. 2, Eq. (4) nicely agrees with numerical data over an extensive range of parameters. Note that these asymptotic results, as well as the initial decay laws as given by Eq. (3), are valid for the dynamics of *any* initial separable state, not just of a computational state. This is illustrated for two relevant cases in Fig. 3.

Initial entangled states.— The analysis may be extended to the dynamics of arbitrarily entangled initial states.

Consider a state in the central band containing only bipartite entanglement first, for instance

$$|\psi_0(n_B)\rangle = \overbrace{|01 \dots 01\rangle}^{n-2n_B} \otimes \left[\frac{1}{\sqrt{2}}(|01\rangle + |10\rangle) \right]^{\otimes n_B}, \quad (5)$$

where n_B is the number of Bell pairs, $n_B = 0$ recovering the fully separable case. The local purity evolution is depicted in Fig. 3. Reflecting the fact that P_1 is sensitive to all correlations between spins, the initial value is lower the larger n_B , $P_1(0) = 1 - 2n_B/n$, using Eq. (1). For $t > 0$, $P_1(t)$ decays similarly to the separable case, two distinct dynamical regimes emerging for $n_B = 0, 1, 2, 3$. As expected, data corresponding to a given regime approximately fall on the same curve once rescaled by $P_1(0)$ (Fig. 3, inset). This may be quantitatively understood by studying the evolution of the bi-local purity defined in Eq. (2). By construction, P_2 is insensitive to any pairwise correlation present in the state (5), effectively mapping the analysis back to the separable case $n_B = 0$. $P_2(t)$ is depicted in the inset of Fig. 4. Clearly, $P_2(0) = 1$ irrespective of n_B . The time decay then follows the two regimes predicted by (3), again reflecting the underlying structure of the LDOS (see Fig. 4).

As a representative example of an initial state containing genuine multipartite entanglement, we focus on a so-called $|\mathbb{W}\rangle$ state that is, an equally weighted superposition with equal phases of the $N_B(1) = n$ states with z -magnetization one. Within our disorder model, $|\mathbb{W}\rangle$ is automatically protected against the effects of H_δ, H_J as long as the coupling between different bands remains small, as assumed so far. Indeed, the local purity remains almost constant (data not shown). Thus, to analyze how the (tripartite) correlations contained in a $|\mathbb{W}\rangle$ are affected by static random imperfections we set $\Delta = 0$ [21]. Again, the same qualitative picture arises, with two distinct dynamical regimes (inset of Fig. 3) and two different scalings of critical decay times t_c (Fig. 4) [22].

Conclusions.— We have established the existence of distinctive dynamical signatures in the evolution of multipartite entanglement in a quantum many-body system subject to static disorder. While a more systematic analysis is certainly desirable, we expect our main conclusions to prove valid under more general conditions, including different dimensionality and/or model Hamiltonians, as well as higher-spin systems. Beside reinforcing the usefulness of the GE notion as a diagnostic framework for complex quantum systems, the deep connections between GE, LDOS, and fidelity decay emerging from our work are likely to have broader implications across the fields of quantum information and quantum chaos, further stimulating crosstalk between the two communities.

We thank R. Fazio, G. Ortiz, L. F. Santos, and Y. Weinstein for enlightening discussions. Partial support from the IST-SQUBIT2, from IBM (Faculty Awards 2005), and from Constance and Walter Burke through their Spe-

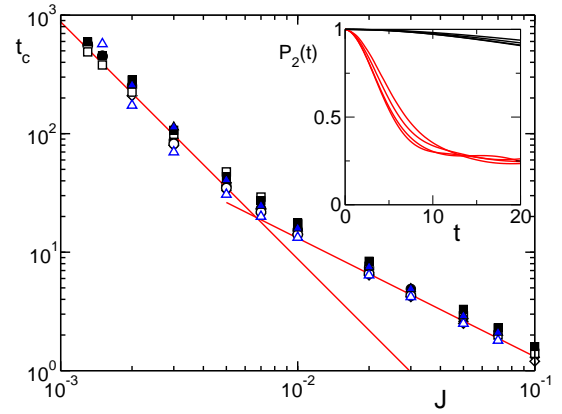


FIG. 4: Purity critical time t_c as a function of J for $\delta = 0.1$ for different initial states, $n_B = 1$ (circles), $n_B = 2$ (squares), $n_B = 3$ (diamonds), $|\mathbb{W}\rangle$ (blue triangles,) and different purity measures: $P_1(t)$ (empty) and $P_2(t)$ (full). Inset: $P_2(t)$ vs time in the FGR regime (black lines) and in the ergodic regime (red lines) for different initial states with $n_B = 0, 1, 2, 3$.

cial Projects Fund in QIS is gratefully acknowledged.

* Corresponding author. E-mail: monta@sns.it

- [1] S. Sachdev, *Quantum Phase Transitions* (Cambridge University Press, Cambridge, UK, 1999).
- [2] T. Guhr, A. Müller-Groeling, and H. A. Weidenmüller, Phys. Rep. **299**, 189 (1998).
- [3] *Forsch. Phys.* **48**, No. 9–11, Special Focus Issue on *Experimental Proposals for Quantum Computation* (2000).
- [4] B. Georgeot and D. L. Shepelyansky, Phys. Rev. E **62**, 3504 (2000); *ibid.* **62**, 6366 (2000).
- [5] V. V. Flambaum, Aust. J. Phys. **53**, 489 (2000).
- [6] G. Benenti *et al*, Phys. Rev. Lett. **87**, 227901 (2001).
- [7] G. P. Berman *et al*, Phys. Rev. E **64**, 056226 (2001).
- [8] L. F. Santos, G. Rigolin, and C. O. Escobar, Phys. Rev. A **69**, 042304 (2004).
- [9] C. Mejia-Monasterio *et al*, Phys. Rev. A **71**, 062304 (2005).
- [10] The LDOS describes the profile of an eigenstate of an unperturbed quantum system over the eigenbasis of the perturbed version of the same quantum system.
- [11] See e.g. G. Benenti and G. Casati, Phys. Rev. E **65**, 066205 (2002), T. Prosen, Th. H. Seligman, and M. Znidaric, Progr. Theor. Phys. Suppl. **150**, 200 (2003), and references therein.
- [12] S. Montangero, G. Benenti, and R. Fazio, Phys. Rev. Lett. **91**, 187901 (2003).
- [13] W. Wootters, Phys. Rev. Lett. **80**, 2245 (1998).
- [14] H. Barnum *et al*, Phys. Rev. A **68**, 032308 (2003); H. Barnum *et al*, Phys. Rev. Lett. **92**, 107902 (2004).
- [15] R. Somma *et al*, Phys. Rev. A **70**, 042311 (2004).
- [16] I. M. Lifshits, S. A. Gredeskul, and L. A. Pastur, *Introduction to the Theory of Disordered Systems* (Wiley, New York, 1988).
- [17] D. Meyer and N. R. Wallach, J. Math. Phys. **43**, 4273 (2002).
- [18] G. K. Brennen, Quantum Inf. Comput. **3**, 619 (2003).

- [19] P. Facchi *et al*, Phys. Rev. A **71**, 060306(R) (2005).
- [20] Y. S. Weinstein *et al*, Quant. Inf. Proc. **1**, 439 (2003).
- [21] We could alternatively choose $J > \Delta$.
- [22] We also verified the evolution of $P_1(t)$ for an initial $|\text{GHZ}\rangle$ state. However, the entanglement present in this state

is stable against the disorder induced by H , leading to nearly no time evolution. This is due to the fact that $|\text{GHZ}\rangle$ is a superposition of two states lying at the extremes of the energy spectrum, practically decoupled from the rest.